

RESEARCH ARTICLE

10.1002/2017JG004008

Key Points:

- Diffuse radiation is an important driver of the photosynthetic seasonality in Amazon evergreen forests
- A new diffuse fraction-based two-leaf GPP model simulates the photosynthetic seasonality of Amazon evergreen forests

Supporting Information:

- Supporting Information S1

Correspondence to:

H. Yan,
yanhaon@hotmail.com

Citation:

Yan, H., Wang, S.-Q., da Rocha, H. R., Rap, A., Bonal, D., Butt, N., ... Shugart, H. H. (2017). Simulation of the unexpected photosynthetic seasonality in Amazonian evergreen forests by using an improved diffuse fraction-based light use efficiency model. *Journal of Geophysical Research: Biogeosciences*, 122, 3014–3030. <https://doi.org/10.1002/2017JG004008>

Received 20 JUN 2017

Accepted 29 OCT 2017

Accepted article online 6 NOV 2017

Published online 20 NOV 2017

Simulation of the Unexpected Photosynthetic Seasonality in Amazonian Evergreen Forests by Using an Improved Diffuse Fraction-Based Light Use Efficiency Model

Hao Yan^{1,2} , Shao-Qiang Wang³, Humberto R. da Rocha⁴, Alexandru Rap⁵ , Damien Bonal⁶, Nathalie Butt⁷ , Natalia Restrepo Coupe^{8,9} , and Herman H. Shugart²

¹National Meteorological Center, China Meteorological Administration, Beijing, China, ²Environmental Sciences Department, University of Virginia, Charlottesville, VA, USA, ³Key Laboratory of Ecosystem Network Observation and Modeling, Institute of Geographic Sciences and Natural Resources Research, Chinese Academy of Sciences, Beijing, China, ⁴Departamento de Ciências Atmosféricas, Universidade de São Paulo, São Paulo, Brazil, ⁵School of Earth and Environment, University of Leeds, Leeds, UK, ⁶INRA UMR Ecologie et Ecophysiologie Forestières, Champenoux, France, ⁷School of Biological Sciences, University of Queensland, Brisbane, Queensland, Australia, ⁸Department of Ecology and Evolutionary Biology, University of Arizona, Tucson, AZ, USA, ⁹Plant Functional Biology and Climate Change Cluster, University of Technology Sydney, Sydney, New South Wales, Australia

Abstract Understanding the mechanism of photosynthetic seasonality in Amazonian evergreen forests is critical for its formulation in global climate and carbon cycle models. However, the control of the unexpected photosynthetic seasonality is highly uncertain. Here we use eddy-covariance data across a network of Amazonian research sites and a novel evapotranspiration (E) and two-leaf-photosynthesis-coupled model to investigate links between photosynthetic seasonality and climate factors on monthly scales. It reproduces the GPP seasonality ($R^2 = 0.45\text{--}0.69$) with a root-mean-square error (RMSE) of $0.67\text{--}1.25 \text{ g C m}^{-2} \text{ d}^{-1}$ and a Bias of $-0.03\text{--}1.04 \text{ g C m}^{-2} \text{ d}^{-1}$ for four evergreen forest sites. We find that the proportion of diffuse and direct sunlight governs the photosynthetic seasonality via their interaction with sunlit and shaded leaves, supported by a proof that canopy light use efficiency (LUE) has a strong linear relationship with the fraction of diffuse sunlight for Amazonian evergreen forests. In the transition from dry season to rainy season, incident total radiation (Q) decreased while LUE and diffuse fraction increased, which produced the large seasonal increase ($\sim 34\%$) in GPP of evergreen forests. We conclude that diffuse radiation is an important environmental driver of the photosynthetic seasonality in tropical Amazon forests yet depending on light utilization by sunlit and shaded leaves. Besides, the GPP model simulates the precipitation-dominated GPP seasonality ($R^2 = 0.40\text{--}0.69$) at pasture and savanna sites. These findings present an improved physiological method to relate light components with GPP in tropical Amazon.

Plain Language Summary Understanding the mechanism of photosynthetic seasonality in Amazonian evergreen forests is critical for its formulation in global climate and carbon cycle models. However, the control of the unexpected photosynthetic seasonality is highly uncertain. Here we use eddy-covariance data across a network of Amazonian research sites and a novel evapotranspiration (E) and two-leaf-photosynthesis-coupled model to investigate links between photosynthetic seasonality and climate factors on monthly scales. It reproduces the GPP seasonality ($R^2 = 0.45\text{--}0.69$) for four evergreen forest sites. We find that the proportion of diffuse and direct sunlight governs the photosynthetic seasonality via their interaction with sunlit and shaded leaves, supported by a proof that canopy light-use efficiency (LUE) has a strong linear relationship with the fraction of diffuse sunlight for Amazonian evergreen forests. We conclude that diffuse radiation is an important environmental driver of the photosynthetic seasonality in tropical Amazon forests yet depending on light utilization by sunlit and shaded leaves. Besides, the GPP model simulates the precipitation-dominated GPP seasonality ($R^2 = 0.40\text{--}0.69$) at pasture and savanna sites. These findings present an improved physiological method to relate light components with GPP in Amazon.

1. Introduction

Amazonian tropical forests store 70–80 petagrams (10^{15} g) of carbon in biomass (Houghton et al., 2001), and their photosynthetic and water metabolism regulates regional and global climate (Davidson et al., 2012; Guan et al., 2015). Flux tower measurements and remote sensing observations indicate that Amazonian

evergreen forests have an unexpected photosynthetic seasonality with increased productivity (“Green up”) during dry seasons (Saleska et al., 2003), potentially from deep roots allowing forests to avoid water stress (Bi et al., 2015; Goulden et al., 2004; Huete et al., 2006), implying that light is more limiting than water (Nemani et al., 2003).

Numerous hypotheses have been proposed to account for the photosynthetic seasonality, naturally from the view point of biology or climate. Leaf phenological hypothesis (De Weirtdt et al., 2012; Doughty & Goulden, 2008; Restrepo-Coupe et al., 2013; Wu, Albert, et al., 2016) attributes the gross primary productivity (GPP) seasonality to leaf age classes (i.e., young, mature, and old), and corresponding photosynthetic capacity (PC), for example, new leaf growth in dry season, shifting canopy composition toward younger and more light use efficient leaves, produces large GPP increases in dry season. Light-controlled phenology hypothesis (Kim et al., 2012) assumes that the leaf litterfall increases linearly with an increase of incoming total radiation. Forest structure hypothesis (Morton et al., 2016) emphasizes the canopy structure and direct/diffuse illumination in generating diurnal and seasonal variability of light utilization in Amazon forests by using a three-dimensional (3-D) canopy radiation transfer model. Hydroclimatic hypothesis (Guan et al., 2015) concludes that water availability dominates vegetation seasonality in tropical forests.

Most dynamic global vegetation models poorly capture the annual cycle of GPP of Amazonian evergreen forests (Restrepo-Coupe et al., 2017). The mechanisms and controls on photosynthetic seasonality are unresolved. This limits prediction of tropical forest’s responses to climate change and produces large uncertainties in the contemporary carbon balance of tropical forests (Morton et al., 2014; Wu, Albert, et al., 2016).

Worldwide, canopy light use efficiency (LUE) increases as diffuse radiation increases (Cirino et al., 2014; Gu et al., 2002; Mercado et al., 2009; Roderick et al., 2001). Surface radiation measurements in Amazonian evergreen forests show reciprocal variation of diffuse radiation and total radiation in rainy and dry seasons (Butt et al., 2010). Except for the diffuse radiation, statistics analysis has revealed that other climate factors such as incident photosynthetically active radiation (PAR), precipitation, air temperature, and vapor pressure deficit (VPD) do not control GPP seasonality (Wu, Albert, et al., 2016; Wu, Guan, et al., 2016). Here we inspect the hypothesis that diffuse radiation controls the photosynthetic seasonality in Amazonian tropical forests and implements a biophysical model apprehending its physical mechanism. GPP seasonality in Amazonian is a question rooted in LUE according to the big-leaf LUE theory (Monteith, 1972),

$$GPP = LUE \times PAR \times FPAR \tag{1}$$

where FPAR is the fraction of PAR absorbed by the canopy. However, the big-leaf GPP model is not appropriate for analyzing the impact of diffuse radiation on GPP due to disregarding the difference of diffuse and direct sunlight in light use efficiency.

Our aim is to investigate whether light components are the dominant climatic factor driving GPP seasonality in Amazon evergreen forests. Thus, an improved Diffuse fraction-based two-leaf Terrestrial Ecosystem Carbon flux (DTEC) GPP model was adopted by this study, which separates sunlight into its diffuse and direct components and computes their interaction in a simplified two-leaf canopy structure adopted from the TL-LUE GPP model (He et al., 2013). It also considers the impact of water stress by using a precipitation-driven evapotranspiration (*E*) model (Yan et al., 2012). The sections below present: (1) correlation analysis between diffuse fraction and canopy light use efficiency at four Amazon evergreen forest sites; (2) evaluation of the diffuse fraction model with observed diffuse fraction; (3) evaluation of the DTEC GPP model in simulating GPP seasonality against flux tower GPP at Amazon evergreen forest sites as well as its performance at pasture and savanna sites, (4) sensitivity analysis of DTEC GPP and LUE to leaf area index (LAI) data at K67 evergreen forest site, and (5) evaluation of estimated *E* against flux tower *E*.

2. Methods

2.1. Canopy Light Use Efficiency, Radiation Use Efficiency, and Diffuse Fraction

$$LUE = \frac{GPP}{(PAR \times FPAR)} \tag{2}$$

$$RUE = \frac{GPP}{PAR} \tag{3}$$

where GPP is gross ecosystem production, PAR is the incident photosynthetically active radiation, FPAR is the fraction of PAR absorbed by the canopy.

Diffuse fraction (D_f) is defined as the ratio of diffuse radiation (Q_{dif}) to incident total radiation (Q),

$$D_f = Q_{dif}/Q \quad (4)$$

2.2. Summary of the DTEC GPP Model

The E -coupled two-leaf-GPP model (DTEC) is defined as

$$GPP = (\epsilon_{msu} \times APAR_{sun} + \epsilon_{msh} \times (0.25 + 0.75 \times D_f^{P_w}) \times APAR_{shd}) \times W_\epsilon \times T_\epsilon \quad (5)$$

where ϵ_{msu} and ϵ_{msh} are maximum LUE of 1.11 and 4.35 ($g\ C\ MJ^{-1}$) for sunlit and shaded leaves, D_f is diffuse fraction and P_w is 1.8, $APAR_{sun}$ and $APAR_{shd}$ are monthly PAR absorbed by sunlit and shaded leaves, and W_ϵ and T_ϵ are water and temperature stress factors, respectively. $(0.25 + 0.75 \times D_f^{P_w})$ represents the effect of diffuse fraction on LUE for shaded canopy, which scales ϵ_{msh} of shaded leaves to actual LUE of shaded canopy coupled with W_ϵ and T_ϵ . ϵ_{msu} , ϵ_{msh} , and P_w were determined from calibration at the K67 site (see section 2.3).

$$APAR_{sun} = \left[PAR_{dir} \times \frac{\cos(\beta)}{\cos(\theta)} + \frac{PAR_{dif} - PAR_{dif,u}}{LAI} + C \right] \times LAI_{sun} \quad (6)$$

$$APAR_{shd} = \left[\frac{PAR_{dif} - PAR_{dif,u}}{LAI} + C \right] \times LAI_{shd} \quad (7)$$

$$LAI_{sun} = 2 \times \cos(\theta) \times \left[1 - \exp\left(-0.5 \times \Omega \times \frac{LAI}{\cos(\theta)}\right) \right] \quad (8)$$

$$LAI_{shd} = LAI - LAI_{sun} \quad (9)$$

$$PAR_{dif,u} = PAR_{dif} \times \exp\left(-0.5 \times \Omega \times \frac{LAI}{0.537 + 0.025\ LAI}\right) \quad (10)$$

$$C = 0.07 \times \Omega \times PAR_{dir} \times (1.1 - 0.1 \times LAI) \times \exp(-\cos(\theta)) \quad (11)$$

where PAR_{dif} and PAR_{dir} are monthly diffuse and direct radiation of PAR, respectively. $PAR_{dif,u}$ is diffuse radiation under the plant canopy; C represents contribution of multiple scattering of direct radiation to the diffuse radiation (Norman, 1982); β is mean leaf-sun angle and set to 60° for a canopy with spherical leaf angle distribution (Chen et al., 1999); θ is monthly average solar zenith angle at noon; and Ω is clumping index dependent on vegetation types and set to 0.8, 0.9, and 0.8 for evergreen broadleaf forest, grass, and savanna, respectively (He et al., 2013; Zhou et al., 2016). LAI_{sun} and LAI_{shd} are LAI of sunlit leaf and shaded leaf, respectively.

Diffuse radiation PAR_{dif} is estimated from the sky clearness index (SI)-based empirical diffuse fraction model (He et al., 2013),

$$PAR_{dif} = PAR \times D_f \quad (12)$$

$$D_f = 0.7527 + 3.8453 \times SI - 16.316 \times SI^2 + 18.962 \times SI^3 - 7.0802 \times SI^4 \quad (13)$$

$$SI = Q/Q_0 \quad (14)$$

$$Q_0 = S_0 \times \cos(\theta) \quad (15)$$

where SI is sky clearness index, Q is incident total radiation, Q_0 is global solar irradiance at the top of the atmosphere, S_0 is solar constant ($1,367\ W\ m^{-2}$), and θ is solar zenith angle. Cloudiness index (CI; Wu, Albert, et al., 2016) is defined as 1 minus SI,

$$CI = 1 - SI \quad (16)$$

The water stress factor W_ϵ is calculated following the TEC GPP model (Yan et al., 2015),

$$W_\epsilon = \frac{E}{E_{pT}} \quad (17)$$

where E_{pT} is the potential evaporation (Priestley & Taylor, 1972) and E is the actual evapotranspiration calculated from the air-relative humidity-based two-source (ARTS) E model (Yan et al., 2012) that simulates the surface energy balance, soil water balance, and environmental constraints on E with inputs of remotely

Table 1
Parameterization of DTEC Model for Each of the Six Stations

| Parameter | K67 | K83 | RJA | BAN | FNS | PDG |
|---|------|------|------|------|------|------|
| ϵ_{msh} (this study) | 4.35 | 4.35 | 4.35 | 4.35 | 4.35 | 4.35 |
| ϵ_{msu} (this study) | 1.11 | 1.11 | 1.11 | 1.11 | 1.11 | 1.11 |
| T_{min} (°C), Raich et al. (1991) | 2.5 | 2.5 | 2.5 | 2.5 | 1 | -1 |
| T_{max} (°C), Raich et al. (1991) | 47.5 | 47.5 | 47.5 | 47.5 | 48 | 49.5 |
| T_{opt} (°C), Raich et al. (1991) | 27.5 | 27.5 | 27.5 | 27.5 | 30 | 30 |
| Clumping Index (Ω), Zhou et al. (2016) | 0.8 | 0.8 | 0.8 | 0.8 | 0.9 | 0.8 |

sensed LAI, surface meteorological data, and soil texture data. ARTS E model has been evaluated against observed E at 19 flux tower sites (Yan et al., 2012) and applied to diagnostic analysis of interannual variation of global land E (Yan et al., 2013) and global drought monitoring over 1982–2011 (Yan et al., 2014).

The temperature stress factor T_{ϵ} is calculated following the Terrestrial Ecosystem Model (Raich et al., 1991),

$$T_{\epsilon} = \frac{(T_a - T_{\text{min}})(T_a - T_{\text{max}})}{(T_a - T_{\text{min}})(T_a - T_{\text{max}}) - (T_a - T_{\text{opt}})^2} \quad (18)$$

where T_a is the air temperature (°C) and T_{min} , T_{max} , and T_{opt} are minimum, maximum, and optimal temperature for photosynthetic activities, respectively, and their values (Table 1) were adopted from Raich et al. (1991).

2.3. Calibration of the DTEC GPP Model

In the DTEC GPP model, three parameters of ϵ_{msu} , ϵ_{msh} , and P_w (see equation (5)) were determined by using calibration method. As KM67 evergreen forest site features a typical diffuse sunlight-abundant climate without water stress impact even in dry seasons (Goulden et al., 2004), it becomes the optimal site for calibrating D_f -based GPP model.

Driven with Moderate Resolution Imaging Spectroradiometer (MODIS)-derived LAI (Table S1 in the supporting information) and flux tower meteorological data at the KM67 site on a monthly scale, ϵ_{msu} , ϵ_{msh} , and P_w were tuned within a range of 0.5–1.5, 3.0–5.0, and 1.0–2.5, respectively, with a step of 0.01 through calibration process. The optimal values of these parameters (i.e., $\epsilon_{\text{msu}} = 1.11$, $\epsilon_{\text{msh}} = 4.35$, and $P_w = 1.8$) were obtained when the root-mean-square error (RMSE) of calibrated DTEC LUE against flux LUE reached a minimum value of 0.11 (Figure S1), and calibrated DTEC GPP had a similar seasonal variation ($R^2 = 0.45$, $P < 0.0001$) with flux GPP on a monthly scale. Then the calibrated-DTEC model was applied to analyze the GPP seasonality at other sites driven with MODIS-LAI (Table S1), meteorological data, and respective model parameters (Table 1).

Figure S2 shows that canopy LUE and estimated LUE for shaded leaves had seasonal changes, while MODIS LAI for shaded and sunlit leaves as well as estimated LUE for sunlit leaves had no seasonal changes.

3. Materials

3.1. Characteristics of Flux Tower Sites

This study selected six eddy covariance tower sites (Table 2) with monthly continuous data spanning 2 to 3 years from the Brazil flux network (De Gonçalves et al., 2013; Restrepo-Coupe et al., 2013). The sites are the Tapajós National forest near Santarém (K67 and K83 tropical rainforests; Da Rocha et al., 2004; Hutyra et al., 2007; Saleska et al., 2003); the Reserva Jarú (RJA tropical wet and dry forest; Kruijt et al., 2004), the Bananal Island (BAN, seasonally flooded forest-savanna ecotone); the Fazenda Nossa Senhora (FNS pasture; Von Randow et al., 2004) near Ji-Paraná-Rondonia; and the Reserva Pe-de-Gigante in Sao Paulo state (PDG savanna). Their spatial locations are shown in Figure S3. The FNS and PDG sites, covered with pasture and savanna, respectively, suffer water stress in dry seasons while the other four sites are covered with tropical evergreen forest. Dry season is defined with monthly rainfall < 100 mm (De Weirtdt et al., 2012; Wu, Albert, et al., 2016).

Site parameters, including tower height, canopy height, soil texture, and soil depth (Table 2), were adopted to calculate aerodynamic conductance (G_a) and maximum soil available water content (Saxton et al., 1986),

Table 2
Flux Tower Site Characteristics

| ID | K67 | K83 | RJA | BAN | FNS | PDG |
|-------------------|---------------------|----------------------------|-----------------------------|----------------------------|--------------------------|---------------|
| Site name | Santarem Km67 | Santarem Km83 | Reserva Jaru | Javaes River Reserva | Fazenda Nossa Senhora | Pe-de-Gigante |
| Longitude | −54.96 | −54.97 | −61.93 | −50.16 | −62.36 | −47.65 |
| Latitude | −2.86 | −3.02 | −10.08 | −9.82 | −10.76 | −21.62 |
| Tower height (m) | 63 | 64 | 60 | 40 | 8.5 | 21 |
| Biome type | Tropical rainforest | Logged tropical rainforest | Tropical wet and dry forest | Seasonally flooded ecotone | Pasture | Savanna |
| Canopy height (m) | 35 | 35 | 30 | 16 | 0.5 | 12 |
| Sand (%) | 2 | 18 | 80 | 24 | 80 | 85 |
| Silt (%) | 8 | 2 | 10 | 39 | 10 | 12 |
| Clay (%) | 90 | 80 | 10 | 37 | 10 | 3 |
| Soil depth (m) | 15 | 12 | 7 | 15 | 7 | 3.5 |
| MAWC (mm) | 2,000 | 1,800 | 490 | 2,100 | 490 | 210 |
| Data period | 2002–2004 | 2001–2003 | 2000–2002 | 2004–2006 | April 2000 to March 2002 | 2002–2003 |
| Data numbers | 36 | 36 | 36 | 36 | 24 | 24 |

Note. Site name, longitude, latitude, tower height, biome type, canopy height, soil texture, soil depth, maximum soil available water content (MAWC), data period, and data numbers.

which further drove the air-relative humidity-based two-source (ARTS) evapotranspiration (E) model (Yan et al., 2012) coupled with flux tower meteorological data.

3.2. Eddy Covariance Data

Flux tower eddy covariance (EC) data were downloaded from the Large-Scale Biosphere-Atmosphere Experiment in Amazônia, Model Intercomparison Project (LBA-MIP; <http://www.climatemodeling.org/lba-mip/>) protocol spanning daily, 16 day, monthly scales. The EC method measures CO_2 , water, and energy fluxes between terrestrial ecosystem and atmosphere at very high temporal frequency (Baldocchi et al., 2001). EC method directly measures net ecosystem exchange (NEE) not GPP at flux tower sites. Ecosystem respiration is often estimated by using a simple temperature-respiration model. Thus, GPP is calculated from the difference between daytime NEE and daytime respiration (Falge et al., 2002) so that GPP inherits all the uncertainties in the measurement of NEE and in the model for daytime respiration.

Flux tower EC observations were initially used to investigate the relationship of diffuse fraction (D_f) versus canopy light use efficiency (LUE) and radiation use efficiency (RUE) on monthly scales. Second, EC observed climate data, that is, incident total radiation (Q), incident photosynthetically active radiation (PAR), net radiation (R_n), sensible heat flux (H), relative humidity (RH), precipitation (P_r), air temperature (T_a), vapor pressure deficit (VPD), actual vapor pressure, and wind speed (W_s), were adopted to estimate E and GPP following the DTEC GPP model. The estimated GPP, canopy LUE, RUE, and E were evaluated against EC observations on monthly scales.

3.3. Leaf Area Index Data

MODIS-derived monthly LAI data at the six flux tower sites (De Goncalves et al., 2010; Table S1) were used to drive the DTEC GPP model in this study and derive FPAR, according to a LAI-based simple exponent equation (He et al., 2013), for calculating canopy LUE. The MODIS LAI products are retrieved from MODIS surface reflectances at up to seven spectral bands at 1 km spatial resolution by using a three-dimensional canopy radiative transfer model and evaluated against field-measured FPAR and LAI (Myneni et al., 2002; Yang et al., 2006). In addition, the camera-derived monthly LAI data at site of K67 (Wu, Albert, et al., 2016; Table S1) was used to drive the DTEC GPP model so as to evaluate the impact of LAI data on GPP seasonality.

4. Results

4.1. Evaluation of the Diffuse Fraction Model With Observed Diffuse Fraction on Monthly Scales

As the application of DETC GPP model in this study depended on monthly D_f data estimated from the empirical D_f model (He et al., 2013) originally derived for daily scale data in China, the D_f model was evaluated against monthly D_f derived from diffuse and total radiation observations available at three Amazon sites.

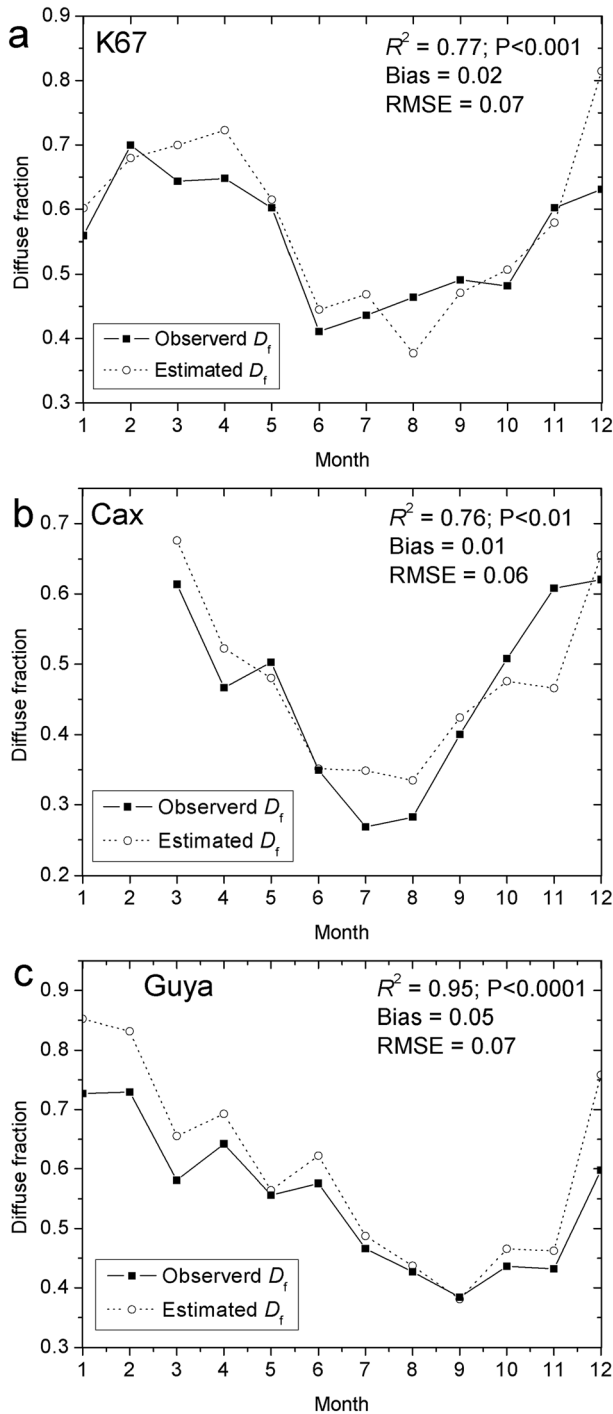


Figure 1. Observed and estimated monthly D_f at (a) K67 in 2005, (b) CAX in 2005, and (c) Guya in 2009.

They are K67 site (Restrepo-Coupe et al., 2013) in 2005, CAX site (Caxiuana, Brazil; 1.738°S, 51.453°W; Butt et al., 2010) in 2005, and Guya site (French Guiana; 5.280°N, 52.926°W; Bonal et al., 2008) in 2009.

Figure 1 shows that the D_f model simulated monthly variations of D_f observed at three Amazon sites with error statistics of $R^2 = 0.76$ – 0.96 , Bias = 0.01–0.05, and RMSE = 0.06–0.07; that is, it was a reliable method to estimate monthly D_f that in turn can be applied to explore the impact of diffuse light on LUE. Note that the diffuse radiation data at K67 site was observed in 2005.

4.2. Diffuse Radiation Drives Seasonality of Light Use Efficiency and GPP in Amazon Evergreen Forests

Canopy LUE was calculated from flux tower GPP, PAR, and MODIS derived-FPAR data. In case of no observations of diffuse radiation accompanying the flux tower data used in this study, the DTEC model adopted the sky clearness index (SI)-based D_f model (He et al., 2013) to infer diffuse fraction from aggregated total radiation (Q) observed at the surface and global solar irradiance (Q_0) at the top of the atmosphere (see equation (13)) on monthly scales at four forest sites (K67, K83, RJA, and BAN forest sites).

Comparing the flux LUE and the diffuse fraction, we find the flux LUE had a significant correlation with diffuse fraction at all four forest sites (determination coefficient $R^2 = 0.72$ – 0.86 ; Figures 2a–2d), which is consistent with observations elsewhere (Choudhury, 2000; Farquhar & Roderick, 2003; Kanniah et al., 2013).

This inspired us to look beyond correlation and to apply a biophysical model, the two-leaf DTEC GPP model, to inspect the degree that light components could control GPP seasonality. The DTEC GPP model reproduced the monthly GPP seasonality ($R^2 = 0.45$ – 0.69 ; Figures 3a–3d), LUE seasonality ($R^2 = 0.68$ – 0.82 ; Figures 4a–4d), and RUE seasonality ($R^2 = 0.67$ – 0.81 ; Figures S4a–S4d) with similar amplitudes to observations from the four forest sites. The separation of diffuse light from direct light produced reliable GPP, LUE, and RUE estimates on monthly scales. We conclude that diffuse radiation was the climatic factor driving GPP seasonality in Amazonian evergreen forests.

Correlation analysis (Table 3) applied to GPP and environmental factors on monthly scales indicates that GPP had a positive relationship with PAR_{dif} but a negative relationship with PAR, T_a , and VPD at two rainforest sites of K67 and K83; that is, PAR, T_a , VPD, and precipitation were not the dominants of GPP seasonality. However, GPP positively correlated with PAR_{dif} as well as water factors (i.e., P_r and RH; $P < 0.0001$) at wet and dry forests (RJA) and seasonally flooded forest in the forest-savanna transition (BAN), which reveals that both PAR_{dif} and water factors contributed to GPP seasonality of evergreen forests at RJA and BAN sites, i.e., water deficiency also decreased GPP in dry season.

In the Amazon, there was a higher diffuse fraction (e.g., up to 0.9 at K67), with more diffuse radiation in wet seasons, and a lower diffuse fraction (e.g., down to 0.55 at K67) along with less diffuse radiation in dry seasons (Figure 4). These produced a distinctive LUE seasonality with a higher LUE (e.g., up to $1.9 \text{ g C MJ}^{-1} \text{ m}^{-2}$ at K67) in rainy seasons but a lower LUE (e.g., down to $1.1 \text{ g C MJ}^{-1} \text{ m}^{-2}$ at K67) in dry seasons (Figure 4). In the transition from dry season to rainy season, incident total radiation (Q) decreased while LUE increased as did D_f , which in concert produced large seasonal increases (~34%) in GPP of evergreen forests (Figures 3a–3d).

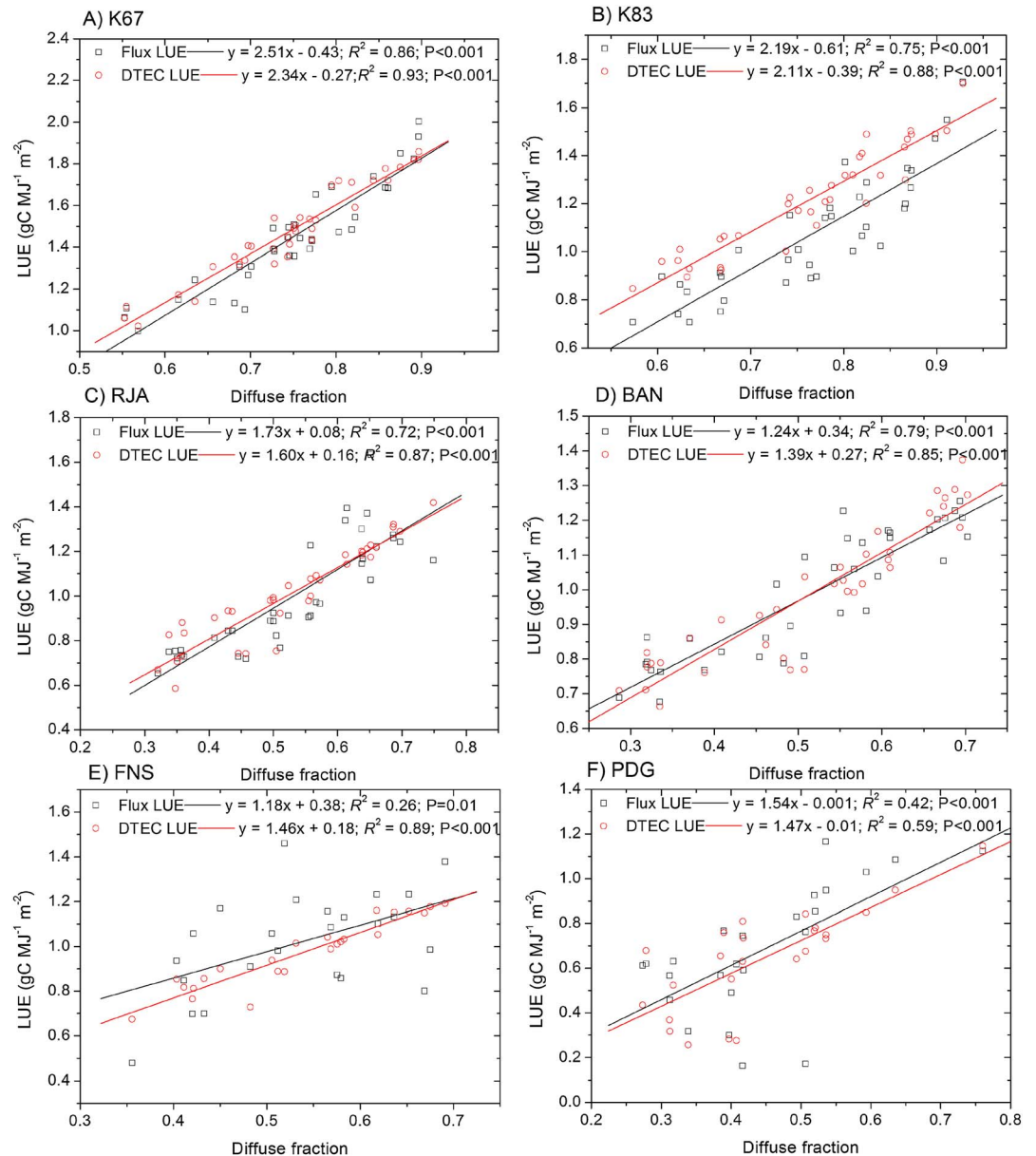


Figure 2. Relationship of observed and estimated canopy light use efficiency (LUE) with diffuse fraction at (a, K67; b, K83; c, RJA; and, d, BAN) four Amazonian forest sites, (e) the FNS pasture site, and (f) the PDG savanna site.

To evaluate the robustness of the impact of diffuse radiation on GPP and exclude the uncertainty from using MODIS-derived FPAR in canopy LUE calculation, we find that observed and estimated RUE correlated well with diffuse fraction at four evergreen forest sites ($R^2 = 0.75\text{--}0.93$; Figures S4a–S4d), implying that canopy RUE, similar to canopy LUE, depends on diffuse fraction in Amazonian evergreen forests.

4.3. Evaluation of the DTEC GPP Model Against Flux Observed GPP at Six Flux Tower Sites

Driven with MODIS-derived LAI and flux tower meteorological data, the DTEC GPP model was applied to all six sites. Estimated GPP as well as LUE and RUE was evaluated against flux observations (shown in Tables 4, S2, S3, respectively).

The GPP statistics (Table 4) show an RMSE of $0.67\text{--}1.25 \text{ g C m}^{-2} \text{ d}^{-1}$, a Bias of $-0.30\text{--}1.04 \text{ g C m}^{-2} \text{ d}^{-1}$, and R^2 of $0.45\text{--}0.69$ for six sites. The LUE statistics (Table S2) give an RMSE of $0.09\text{--}0.21 \text{ g C MJ}^{-1}$, a Bias of

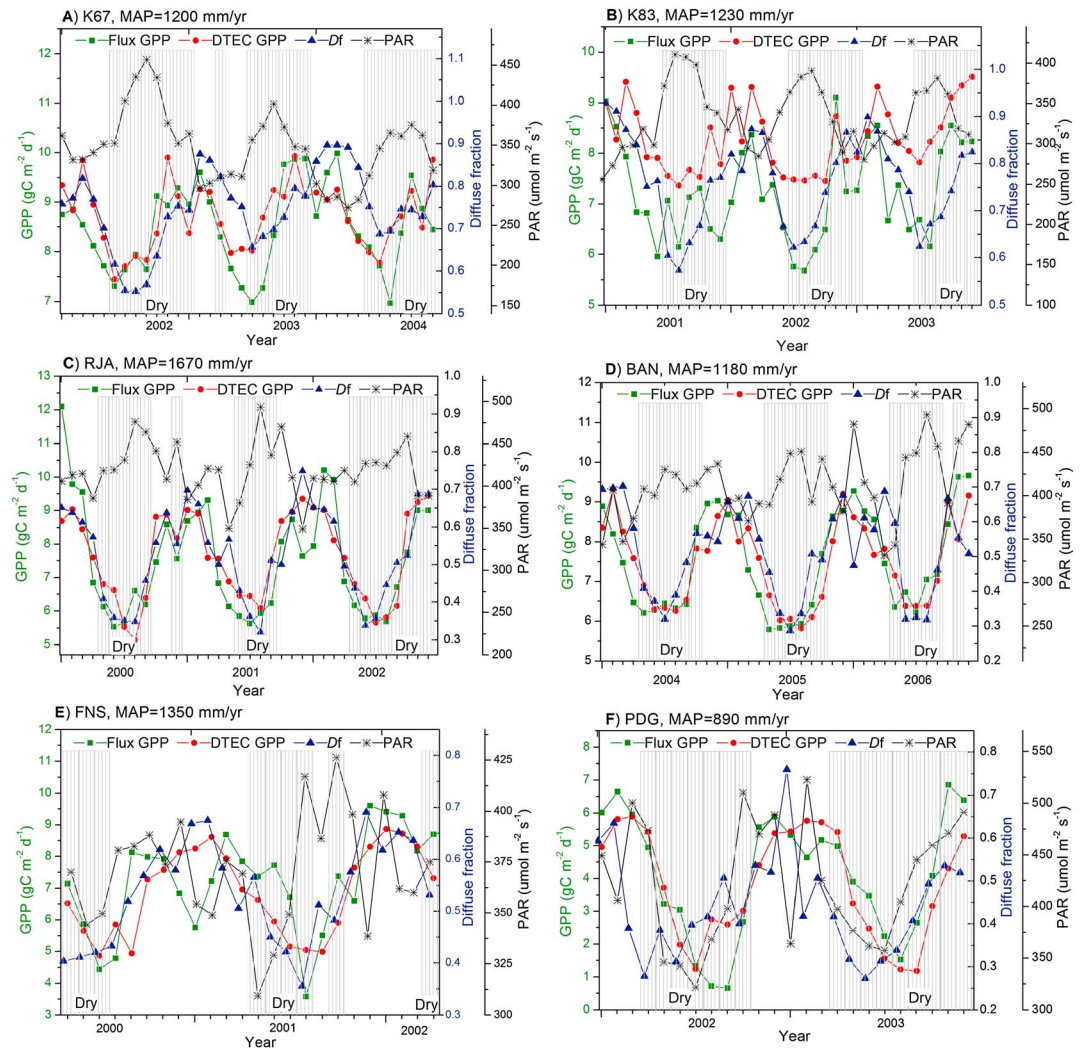


Figure 3. Monthly gross primary production (GPP), diffuse fraction, and incident photosynthetically active radiation (PAR) at (a–d) four forest sites, (e) the FNS pasture site, and (f) the PDG savanna site. MAP is mean annual precipitation. Shade area indicates dry season with monthly rainfall < 100 mm.

–0.05–0.14 g C MJ⁻¹, and R² of 0.29–0.82 for six sites. The RUE statistics (Table S3) indicate an RMSE of 0.08–0.16 g C MJ⁻¹, a Bias of –0.03–0.14 g C MJ⁻¹, and R² of 0.49–0.81 for six sites.

For all data at six sites, Figure 5a shows that estimated DTEC GPP had an RMSE of 1.01 g C m⁻² d⁻¹, a Bias of 0.18 g C m⁻² d⁻¹, and R² of 73 (P < 0.001). Similarly, Figure 5d indicates that estimated canopy LUE had statistics of RMSE = 0.15 g C MJ⁻¹ m⁻², Bias = 0.02 g C MJ⁻¹ m⁻², and R² = 0.79 (P < 0.001) for all data at six sites. In addition, Figures 5b and 5e show that bias of estimated GPP and LUE spread evenly around zero with an increase of diffuse fraction; that is, the DTEC model gave an improved GPP estimation under condition of high diffuse fraction while other GPP models, regardless of impact of diffuse radiation, often tend to underestimate GPP under high diffuse fraction (He et al., 2013). Bias of estimated GPP and LUE (Figures 5c and 5f) shows that there was a weak overestimation of GPP and LUE during dry season months mainly due to an overestimation at K83 (Figure 3b). For all data, estimated GPP was 2.6%, 2.3%, and 3.5% higher than observed GPP on annual, interannual, and monthly scales, respectively. Similarly, estimated LUE was 2.6%, 2.3%, and 3.7% higher than observed LUE on annual, interannual, and monthly scales, respectively. To correctly simulate the impact of diffuse radiation and improve model, more observation work are encouraged to measure diffuse radiation synchronous with other flux tower data in Amazon.

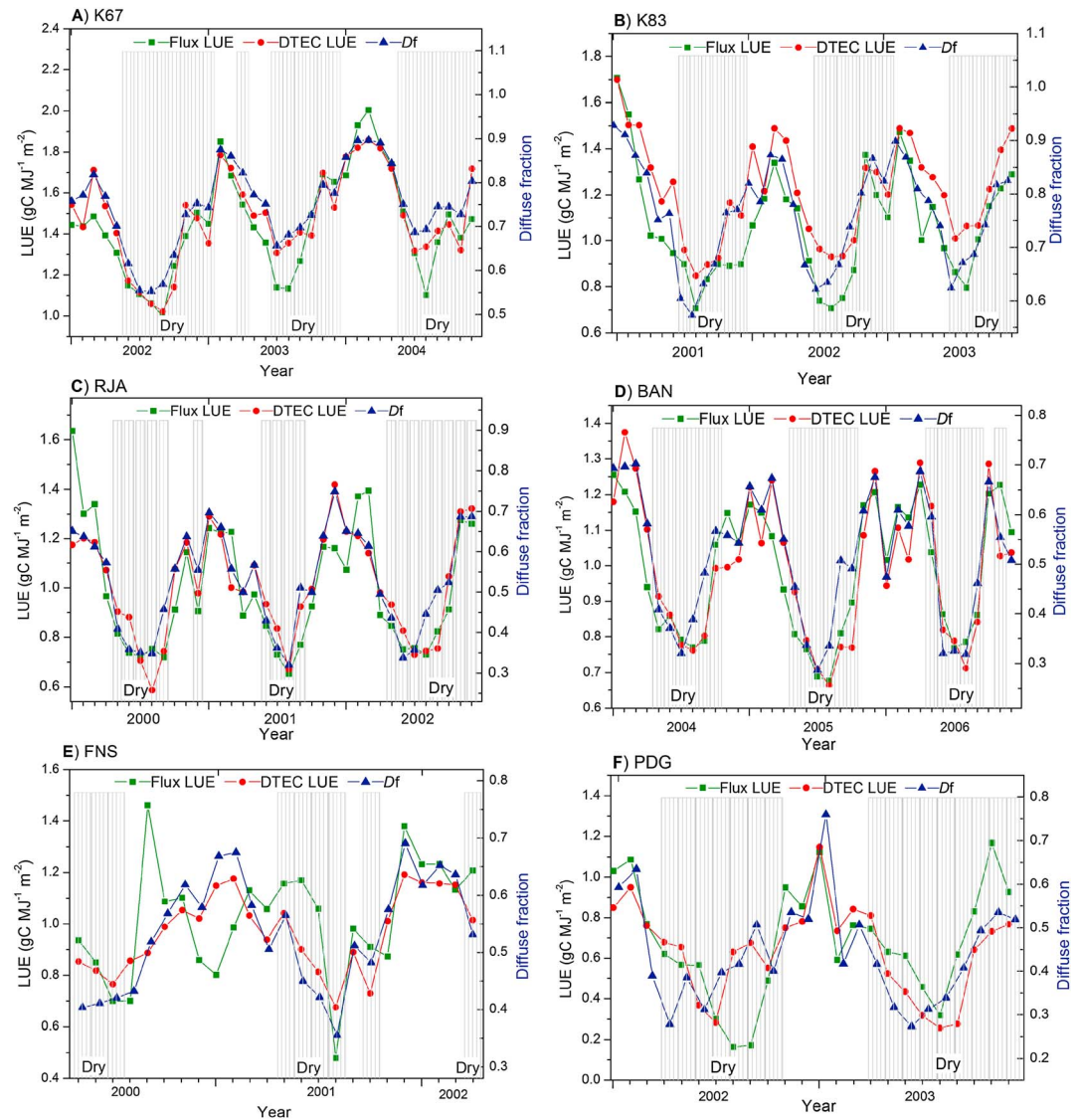


Figure 4. Monthly canopy light use efficiency (LUE) and diffuse fraction (D_f) at (a–d) four forest sites, (e) the FNS pasture site, and (f) the PDG savanna site.

Above error statistics show that the DTEC GPP model simulated the impact of light components as well as water stress on GPP seasonality across forest, pasture, and savanna biomes in tropical Amazonian basin. It suggests that the sunlit and shaded two-leaf GPP modeling structure, due to including the impact of diffuse fraction and water stress factor, was an effective option to explore the impact of light components and other environmental drivers on GPP in Amazonian forests, pasture, and savanna.

Table 3

Correlation Statistics of Correlation Coefficient (R) and Significant Level (P) Between GPP and Environmental Factors on Monthly Scales at Six Sites

| Site | PAR_{dif} | Precipitation | RH | PAR | T_a | VPD |
|------|--------------------------|--------------------------|--------------------------|--------------------------|---------------------------|---------------------------|
| K67 | $(R = 0.64, P < 0.0001)$ | $(R = 0.13, P = 0.45)$ | $(R = 0.15, P = 0.36)$ | $(R = -0.22, P = 0.19)$ | $(R = -0.11, P = 0.54)$ | $(R = -0.10, P = 0.53)$ |
| K83 | $(R = 0.40, P = 0.014)$ | $(R = 0.29, P = 0.08)$ | $(R = 0.42, P = 0.009)$ | $(R = -0.49, P = 0.002)$ | $(R = -0.38, P = 0.02)$ | $(R = -0.28, P = 0.10)$ |
| RJA | $(R = 0.83, P < 0.0001)$ | $(R = 0.81, P < 0.0001)$ | $(R = 0.69, P < 0.0001)$ | $(R = -0.34, P = 0.052)$ | $(R = -0.46, P = 0.0047)$ | $(R = -0.50, P = 0.0017)$ |
| BAN | $(R = 0.81, P < 0.0001)$ | $(R = 0.68, P < 0.0001)$ | $(R = 0.62, P < 0.0001)$ | $(R = -0.11, P = 0.52)$ | $(R = -0.52, P = 0.0013)$ | $(R = -0.61, P < 0.0001)$ |
| FNS | $(R = 0.58, P = 0.003)$ | $(R = 0.44, P = 0.03)$ | $(R = 0.73, P < 0.0001)$ | $(R = -0.34, P = 0.11)$ | $(R = 0.15, P = 0.48)$ | $(R = -0.67, P < 0.001)$ |
| PDG | $(R = 0.65, P < 0.001)$ | $(R = 0.57, P = 0.0037)$ | $(R = 0.81, P < 0.0001)$ | $(R = 0.53, P = 0.008)$ | $(R = 0.47, P = 0.02)$ | $(R = -0.54, P = 0.006)$ |

Note. Positive correlations with $P < 0.05$ are shown in shade area.

Table 4
 Statistics of Estimated Monthly DTEC GPP Versus Flux Tower Observed GPP at Six Flux Tower Sites

| Site | R ² | RMSE | Bias | Linear regression |
|------|------------------|------|---------------|-------------------|
| K67 | 0.45 (P < 0.001) | 0.67 | 0.22 (2.6%) | y = 0.86x + 0.94 |
| K83 | 0.45 (P < 0.001) | 1.25 | 1.04 (14.3%) | y = 0.96x - 0.68 |
| RJA | 0.59 (P < 0.001) | 1.05 | 0.13 (1.7%) | y = 0.97x + 0.09 |
| BAN | 0.69 (P < 0.001) | 0.68 | -0.03 (-0.4%) | y = 0.96x + 0.34 |
| FNS | 0.40 (P < 0.005) | 1.28 | -0.30 (-4.2%) | y = 0.73x + 2.16 |
| PDG | 0.69 (P < 0.001) | 1.07 | -0.24 (-5.9%) | y = 0.95x + 0.45 |

Note. Percent of variance explained (R²), significance level (P), root-mean-square error (RMSE), bias (g C m⁻² d⁻¹), and linear regression equations are used.

4.4. Evaluation of Impact of LAI on GPP Seasonality at K67 Rainforest Site

As Amazonian rainforest features dense vegetation with a relatively stable and high LAI, we investigated the impact of LAI phenology on simulated GPP seasonality at K67 site. We adopted camera-derived monthly LAI, MODIS-derived monthly LAI, and MODIS-derived average LAI of 5.35 at K67 site suggested by LBA-MIP protocol and an assumed constant LAI of 4 (Table S1), combined with the same flux tower climate data at K67 site, to drive the DTEC GPP model. Figure 6a shows that camera-derived monthly LAI demonstrated a seasonality with an increase of about 0.5 from dry season to wet season, while MODIS-derived monthly LAI showed no seasonality.

The estimated GPP_{M_LAI} (driven with MODIS-derived monthly LAI), GPP_{C_LAI} (driven with camera-derived monthly LAI), GPP_{LAI = 5.35}, and GPP_{LAI = 4} were compared with observed GPP at K67 site to evaluate to what degree the LAI seasonality impacted GPP seasonality. Figure 6b indicates that GPP_{M_LAI}, GPP_{C_LAI}, and GPP_{LAI = 5.35} had similar GPP seasonality to the observed flux GPP, while GPP_{LAI = 4} was lower compared with other GPP estimates; that is, the DTEC GPP model was more sensitive to the magnitude of LAI than the seasonality of LAI at K67 site. In this sense, using cloud-contaminated MODIS LAI data did not affect the prediction of GPP seasonality at K67 site.

Figure 6c indicates that canopy LUE_{M_LAI}, LUE_{C_LAI}, LUE_{LAI = 5.35}, and LUE_{LAI = 4} all had similar LUE seasonality to observed flux LUE; that is, estimated LUE was insensitive to the magnitude and seasonality of LAI, which means that LUE was a better index to evaluate the internal correlation between photosynthesis and environmental drivers at Amazonian evergreen forest sites.

Figure 6d shows that RUE_{M_LAI}, RUE_{C_LAI}, and RUE_{LAI = 5.35} had a similar RUE seasonality to observed flux RUE, while RUE_{LAI = 4} had an underestimated RUE value compared with other RUE estimates; that is, estimated RUE like GPP was more sensitive to the magnitude of LAI than the seasonality of LAI. The model sensitivity experiments reveal that LAI phenology played a minor role in seasonality of GPP, LUE, and RUE at the K67 rainforest

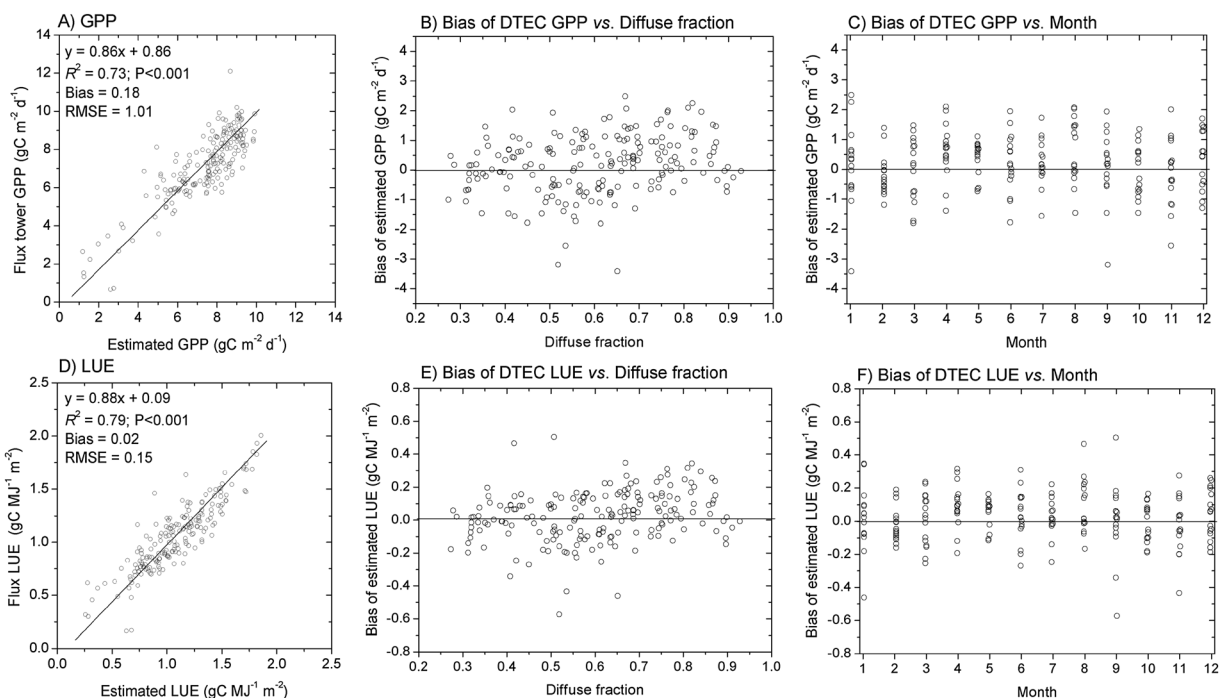


Figure 5. Scatterplots of (a) estimated DTEC GPP versus observed flux tower GPP, (b) bias of DTEC GPP versus diffuse fraction, (c) bias of DTEC GPP versus month, (d) estimated LUE versus observed flux tower LUE, (e) bias of DTEC LUE versus diffuse fraction, and (f) bias of DTEC LUE versus month for all data at six Amazonian sites.

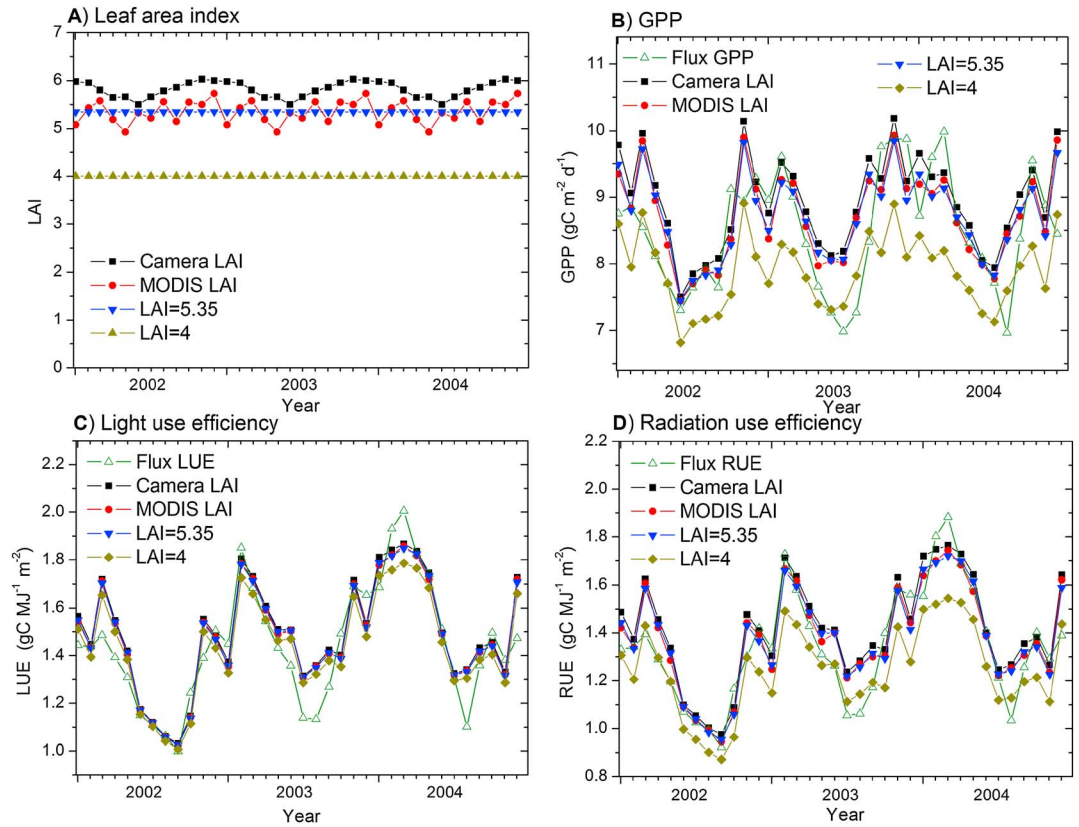


Figure 6. Sensitivity of modeled seasonality of GPP, LUE, and RUE to LAI data at the K67 rainforest site. Time series of (a) camera-derived LAI, MODIS-derived LAI, MODIS-averaged LAI of 5.35, and an assumed constant LAI of 4 used to drive the DTEC GPP model; (b) observed flux GPP and estimated GPP driven with camera LAI, MODIS LAI, constant LAI of 5.35 and 4; (c) observed flux LUE and estimated LUE driven with different LAI data; and (d) observed flux RUE and estimated RUE driven with different LAI data at K67 rainforest site for a period from 2002 to 2004.

site, because common biotic metrics such as LAI have relative amplitudes that are too small to explain the GPP seasonality in Amazonian evergreen forests (Wu, Albert, et al., 2016). Note that we do not address the argument of whether there is LAI seasonality or “Green up” in Amazonian rainforest (Bi et al., 2015; Huete et al., 2006; Morton et al., 2014).

4.5. Sensitivity Analysis of the DTEC GPP Model to Diffuse Radiation

As diffuse radiation played a major role in simulating GPP and LUE seasonality of Amazon forests, sensitivity analysis was applied to the DTEC GPP model driven with different monthly diffuse radiation, defined as a 10% increase (i.e., $1.1 \times D_f$), no change (i.e., $1.0 \times D_f$), and a 10% decrease (i.e., $0.9 \times D_f$), and the other forcing data remaining invariant at the K67 rainforest site for a period from 2002 to 2004.

Figure 7 indicates that both simulated DTEC GPP and canopy LUE were sensitive to diffuse radiation. A 10% increase of diffuse radiation produced an increase of about 14.1% and 14.3% in GPP and LUE, respectively, while a 10% decrease of diffuse radiation caused a decrease of about 11.8% and 12.0% in GPP and LUE, respectively, at the K67 site. In addition, Figure 7 shows that decreases of diffuse radiation also reduced the amplitude of simulated GPP and LUE seasonality.

4.6. Evaluation of Estimated E With Observed Flux Tower E

Figure 8 shows that the estimated E captured seasonal variations of flux tower E at K67 ($R^2 = 0.43$), K83 ($R^2 = 0.46$), RJA ($R^2 = 0.2$), BAN ($R^2 = 0.17$), and PDG ($R^2 = 0.74$). The estimated E had statistics of RMSE = 0.26–0.73 mm d^{-1} and Bias = -0.66 – 0.35 mm d^{-1} for four evergreen forest sites. Evergreen forest and savanna had contrasting response of E to climate in dry season. For example, E increased with an increase of solar radiation in dry season at K67 evergreen forest site featuring radiation-dominated E seasonality and

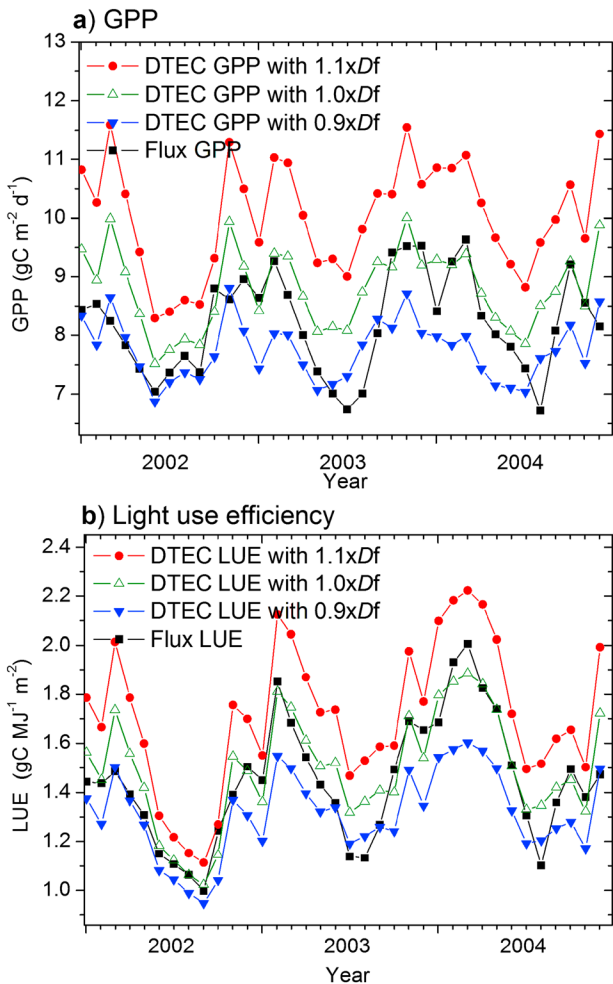


Figure 7. Sensitivity analysis of (a) GPP and (b) LUE to driving forcing of diffuse radiation with $D_f \times 1.1$, $D_f \times 1.0$, and $D_f \times 0.9$ in the DTEC GPP model at the K67 rainforest site for a period from 2002 to 2004, along with observed flux GPP and LUE.

4.8. Uncertainty of Model Calibration

To quantify the associated uncertainty with calibration, this study developed another two-leaf GPP model calibrated with camera-derived LAI at K67 site (Table S1)

$$GPP = (\epsilon_{msu} \times APAR_{sun} + \epsilon_{msh} \times D_f^{P_w} \times APAR_{shd}) \times W_\epsilon \times T_\epsilon \quad (20)$$

where ϵ_{msu} and ϵ_{msh} are maximum LUE of 1.67 and 3.78 ($gC MJ^{-1}$) for sunlit and shaded leaves, D_f is diffuse fraction, and P_w is 1.8.

Evaluation (Table S4) shows that camera LAI-calibrated GPP model had a similar performance to MODIS LAI-calibrated GPP model (Table 4) in terms of R^2 , RMSE, and Bias at six sites. Different calibration data and model structure produced a nonsignificant difference in the model performance.

5. Discussion and Conclusion

Our modeling results reveal that light components acted as the main cause of GPP seasonality in Amazonian evergreen forests, which yet depended on LAI of sunlit and shaded leaves to intercept and utilize PAR. It agrees with previous modeling studies. The forest structure hypothesis (Morton et al., 2016), adopting a three-dimensional (3-D) canopy radiation transfer model, reveals that directional illumination and forest 3-D structure combine to influence seasonal variability in light utilization independent of changes in canopy

plentiful water supply (Figure 8a), while E decreased with a decrease of P_r in dry season at PDG savanna site representing P_r -dominated E seasonality (Figure 8f).

Figure 8e shows that estimated E had P_r -dominated seasonality at the FNS pasture site, that is, dry season exerted drought influence on E . However, estimated E had a poor correlation with observed E ($R^2 = 0.06$). The discrepancy may be due to data quality. According to the surface energy balance, latent heat flux (λE) can be expressed as

$$\lambda E = R_n - G - H, \quad (19)$$

where E is evapotranspiration, λ is the latent heat of vaporization, R_n is net radiation, G is ground heat flux, and H is sensible heat flux. As soil heat flux G can be ignored on monthly time steps in the calculation of E (Allen, 1998). Figure 8e indicates that estimated E reproduced the seasonality of observed $R_n - H$ ($R^2 = 0.89$) that yet had no relationship ($R^2 = 0.06$) with observed E , revealing a serious energy imbalance problem existed at the FNS pasture site due to using the eddy-covariance (EC) method (Leuning et al., 2008).

4.7. Water Controls the GPP Seasonality at Two Water-Stressed Sites in Tropical Amazon

In water-stressed nonforest situations in Amazonian basin, such as the FNS pasture site and the PDG savanna site, observed LUE and RUE had a weaker relationship with diffuse fraction ($R^2 = 0.25-0.42$; Figures 2e, 2f, S4e, and S4f), and light components were not the dominant driver in photosynthetic seasonality at Amazonian water-stressed sites. Table 3 shows that GPP correlated with P_r ($P < 0.05$), RH ($P < 0.0001$), and VPD ($P < 0.01$) at grass and savanna sites (FNS and PDG). Simulated soil moisture (Figures 9a and 9b) further indicates strong water deficit at the two sites in dry seasons, implying that water controls the GPP seasonality at water-stressed sites. The GPP simulations at pasture and savanna sites mean that water deficit as well as light components can be explicitly investigated by using the DTEC-GPP model without extra model tuning or calibration.

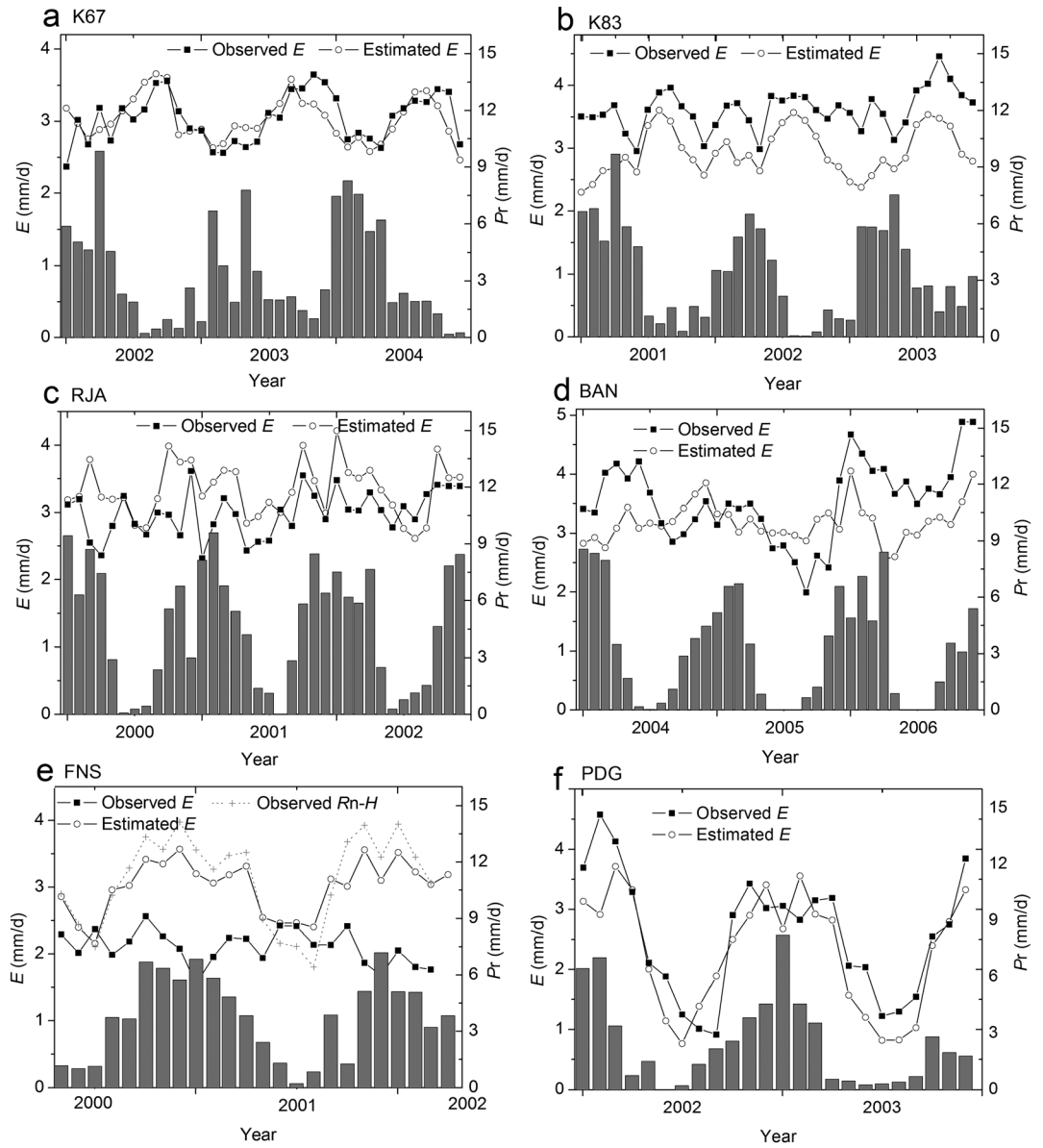


Figure 8. Monthly estimated and observed evapotranspiration (E) and precipitation (P_r) at (a–d) four forest sites, (e) the FNS pasture site, and (f) the PDG savanna site.

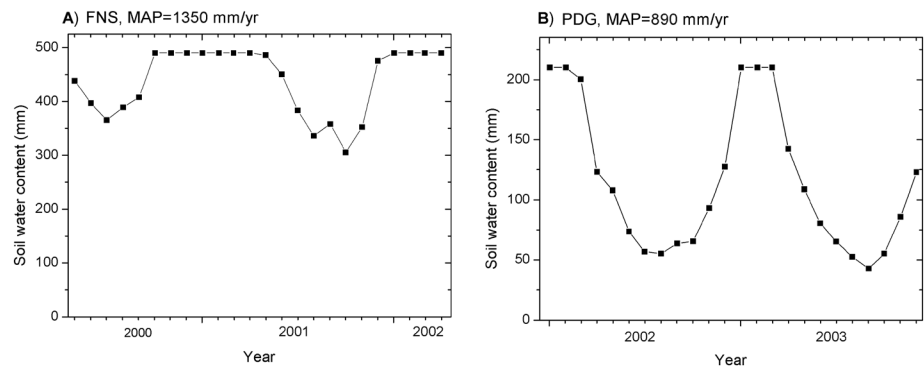


Figure 9. Simulated monthly soil water content at (a) FNS pasture site and (b) PDG savanna site from a soil water balance module coupled in DTEC GPP model. MAP is mean annual precipitation.

phenology (i.e., leaf area and leaf age). This study advanced it by highlighting contributions of diffuse radiation to seasonal variability in LUE but dependent on high LAI values of Amazon evergreen forests.

Similarly, the light-controlled phenology model (Kim et al., 2012) simulates monthly seasonality of net ecosystem productivity (NEP) and litter at the K67 site, based on field observations that leaf litterfall increases linearly with an increase of incoming total radiation. It is consistent with our conclusion that increasing diffuse radiation enhanced LUE and GPP while increasing total radiation, majorly direct radiation, caused the inhibition of canopy LUE and less GPP for Amazon evergreen forests, because total radiation has a reciprocal variation of diffuse radiation (Butt et al., 2010).

However, the phenological hypothesis (Wu, Albert, et al., 2016) underestimates the impact of climate drivers on GPP seasonality in Amazon forests. It attributes the GPP seasonality solely to leaf age classes (i.e., young, mature, and old) and corresponding photosynthetic capacity (PC), for example, new leaf growth produces large GPP increases in dry season. Climate drivers only play a minor role based on low correlation coefficients of GPP versus climatic variables (e.g., cloudiness index (CI) has an R^2 of 0.15–0.57) at four Amazonian forest sites. Following the logic of the phenological hypothesis, a statistical big-leaf LUE model was applied to partitioning controls on Amazon forest photosynthesis between environmental and biotic factors over 7 year observations at the K67 site (Wu, Guan, et al., 2016). Similar result shows that biotic variation in canopy LUE accounts for 63% GPP variability; environmental variation explains only 3% GPP variability at monthly time scales at K67 site ignoring a fact that monthly CI has a significant correlation with LUE and GPP, respectively (Wu, Albert, et al., 2016; Wu, Guan, et al., 2016; this study). A potential concern is expected that the phenological hypothesis does not correctly account for the interaction of diffuse radiation with sunlit and shaded leaves (Morton et al., 2016), and it underestimates the impact of diffuse radiation on GPP seasonality in Amazon forests.

What are the biophysical mechanisms by which light components control GPP seasonality? Plants tend to use diffuse radiation more efficiently than direct radiation (Cheng et al., 2015, 2016) because shaded leaves are not light saturated while sunlit leaves can be light saturated (De Pury & Farquhar, 1997; Gu et al., 2002; Knohl & Baldocchi, 2008; Morton et al., 2016). For optimal efficiency, more nutrients including nitrogen would be allocated to the lower canopy to utilize more light found in the lower canopy in response to higher diffuse radiation (Sellers et al., 1992; Williams et al., 2016). As a result, diffuse radiation enhances leaf photosynthesis capacity relative to more uniform vertical and horizontal PAR redistributions (Li et al., 2014).

Variations of diffuse radiation can be attributed to cloud and aerosol in Amazonian basin. Wet seasons often see more clouds producing more diffuse radiation than that in dry seasons (Butt et al., 2010), but dry seasons experience frequent fire events with large amount of smoke aerosol released (Rap et al., 2015). Smoke increases the diffuse proportion of light. Smoke and its attendant increased-diffuse light have been found to enhance GPP and counteract some of the observed drought effect in dry seasons (Doughty et al., 2010; Rap et al., 2015), as expected from our study. Similarly, the observed 20% increase in carbon uptake (NEE) at two Amazonia flux tower sites is attributed to an enhancement (~50%) in the diffuse fraction of photosynthetic active radiation (PAR) through increases in aerosols and/or clouds (Cirino et al., 2014). We conclude and confirm that GPP and canopy structure are strongly affected by seasonal variations of clouds and aerosols through light components in Amazon forests (Cirino et al., 2014; Roderick et al., 2001).

Nonetheless, Wu, Guan, et al. (2016) recently reported that newly mature leaves, emerging by mid-dry season, have the highest photosynthetic capacity in Amazon evergreen forests, which majorly contributes to GPP increases in dry seasons. We could hypothesize that leaf age distribution as well as LAI seasonality could be an acclimated response to the seasonality of light components for Amazonian evergreen forests. It is well known that plant gets acclimated to its surrounding climate, i.e., climate factors dominate the GPP seasonality with one climatic factor often playing the dominant role. For example, temperature controls GPP seasonality in cold zones while precipitation dominates GPP seasonality in arid zones. Our results suggest that diffuse radiation was the climatic factor dominating GPP seasonality in tropical rainforests.

How do we reconcile disputes of the leaf phenology hypothesis, the diffuse radiation hypothesis, and the hydroclimatic hypothesis? GPP represents utilization of climatic resources by plant canopy through photosynthesis. On a global scale, climate controls global distribution of biome. Phenology variation of plant depends on regional climate (i.e., PAR, PAR_{diff}, D_f , T_a , and P_f) as a result of acclimatization. In this sense, leaf phenology (e.g., leaf age distribution and LAI) synchronizes with and dominates GPP seasonality not only

for tropical evergreen forests as shown by Wu, Albert, et al. (2016) and Wu, Guan, et al. (2016) but also for other biome types.

Thus, those opposite hypothesis about GPP seasonality of tropical rainforests can be reconciled from the viewpoint that climate and plant phenology jointly control seasonal variations in GPP. The leaf phenological hypothesis tries to explain GPP seasonality from the view of plant itself (i.e., plant biology) and attributes GPP seasonality to leaf age and corresponding photosynthetic capacity of Amazon forests.

In addition, the diffuse-radiation hypothesis attributes the GPP seasonality of rainforests to certain climate factors, which is consistent with the forest structure hypothesis (Morton et al., 2016) and the light-controlled phenology hypothesis (Kim et al., 2012). Thus, there is no need to counterpose contributions of leaf phenology and climate factors to GPP seasonality in Amazon forests.

With regard to Amazon pasture and savanna sites, water stress dominated plant phenology and GPP seasonality. However, in Amazon wet and dry forests and forest-savanna ecotone, water stress and diffuse-radiation jointly dominated GPP seasonality complying with the hydroclimatic hypothesis (Guan et al., 2015). We conclude that climate interacts with phenology to control seasonal variations in GPP, but climatic dominants of GPP seasonality vary with biome types.

Accurate leaf phenology data plus knowledge of climatic dominant is bound to improve simulations of GPP seasonality on large spatial scales. However, why do we build GPP model based on LAI data instead of leaf age data? Large uncertainties still exist in the leaf age phenology and its relationship with photosynthetic capacity. Amazon forest observations reported two greening periods of leaf development and the photoperiodic control of leaf phenology (i.e., dormancy, leaf flushing, and flowering) near the equator (Borchert et al., 2015; Calle et al., 2010). For example, half of the observed 54 rainforest species flush in both January and July, that is, two greening periods, in Manaus, Brazil (Borchert et al., 2015). Similarly, microwave remote sensing captures the double annual cycles of leaf flushing in tropical Africa evergreen forests synchronous with annual bimodal changes of the insolation intensity at the top of the atmosphere, which suggests that plant phenology decouples from canopy photosynthetic capacity in tropical evergreen forests (Guan et al., 2013), arguing against the phenological hypothesis (Wu, Albert, et al., 2016) that synchronization of leaf phenology among leaf flushing species drives forest productivity seasonality. The uncertainty and scarcity of leaf age observations limit its application in estimating GPP on a global scale to date.

The DTEC-GPP model can be easily applied because LAI and climate data, as routine parameters, have been adopted by LUE models to simulate GPP seasonality in middle and high-latitude zones (He et al., 2013; Yan et al., 2015). Leaf age is seldom considered in current remote sensing-based LUE models. Although uncertainties still exist in flux tower data and remote sensing LAI data, they do not affect the main conclusion in this study.

We find that GPP seasonality of rainforest, wet and dry forest, pasture, and savanna can be explained by certain climate factors coupled with LAI data in the Amazonian tropical basin. A demonstration of linking light components with LUE supplies a reliable method, coupled in climate-carbon flux models, to predict GPP and its responses to climatic changes. The work also highlights the importance of diffuse radiation as an independent environmental driver in understanding and modeling the GPP seasonality as well as vegetation-climate feedbacks. Accordingly, most GPP-related ecological processes including carbon sink, biomass accumulation, and leaf litterfall, and their responses to climate change need reinvestigation. This is likely to be so in plant response to global dimming or brightening due to changes in aerosol concentration and cloudiness (Mercado et al., 2009; Wild, 2012).

Acknowledgments

We thank the flux site investigators for providing their data through The Large-Scale Biosphere-Atmosphere Experiment in Amazônia, Model Intercomparison Project (LBA-MIP) protocol (<http://www.climatemodeling.org/lba-mip/>) and Climatic Research Unit, University of East Anglia for sharing CRU 3.23 time series data (<http://badc.nerc.ac.uk/home/>). This work was supported by National Natural Science Foundation of China (41571327 and 41171284) and NASA grants to H. H. Shugart: 10-CARBON10-0068 and Climate Change/09-IDS09-116.

References

- Allen, R. G. (1998). *Crop evapotranspiration: guidelines for computing crop water requirements*. Rome: Food and Agriculture Organization of the United Nations.
- Baldocchi, D., Falge, E., Gu, L., Olson, R., Hollinger, D., Running, S., ... Wofsy, S. (2001). FLUXNET: A new tool to study the temporal and spatial variability of ecosystem-scale carbon dioxide, water vapor, and energy flux densities. *Bulletin of the American Meteorological Society*, 82, 2415–2434. [https://doi.org/10.1175/1520-0477\(2001\)082%3C2415:fantts%3E2.3.co;2](https://doi.org/10.1175/1520-0477(2001)082%3C2415:fantts%3E2.3.co;2)
- Bi, J., Knyazikhin, Y., Choi, S., Park, T., Barichivich, J., Ciais, P., ... Myneni, R. B. (2015). Sunlight mediated seasonality in canopy structure and photosynthetic activity of Amazonian rainforests. *Environmental Research Letters*, 10(6). <https://doi.org/10.1088/1748-9326/10/6/064014>
- Bonal, D., Bosc, A., Ponton, S., Goret, J.-Y., Burban, B., Gross, P., ... Granier, A. (2008). Impact of severe dry season on net ecosystem exchange in the Neotropical rainforest of French Guiana. *Global Change Biology*, 14(8), 1917–1933. <https://doi.org/10.1111/j.1365-2486.2008.01610.x>

- Borchert, R., Calle, Z., Strahler, A. H., Baertschi, A., Magill, R. E., Broadhead, J. S., ... Muthuri, C. (2015). Insolation and photoperiodic control of tree development near the equator. *New Phytologist*, 205(1), 7–13. <https://doi.org/10.1111/nph.12981>
- Butt, N., New, M., Malhi, Y., Da Costa, A. C. L., Oliveira, P., & Silva-Espejo, J. E. (2010). Diffuse radiation and cloud fraction relationships in two contrasting Amazonian rainforest sites. *Agricultural and Forest Meteorology*, 150(3), 361–368. <https://doi.org/10.1016/j.agrformet.2009.12.004>
- Calle, Z., Schlumpberger, B. O., Piedrahita, L., Leftin, A., Hammer, S. A., Tye, A., & Borchert, R. (2010). Seasonal variation in daily insolation induces synchronous bud break and flowering in the tropics. *Trees*, 24(5), 865–877. <https://doi.org/10.1007/s00468-010-0456-3>
- Chen, J. M., Liu, J., Cihlar, J., & Goulden, M. L. (1999). Daily canopy photosynthesis model through temporal and spatial scaling for remote sensing applications. *Ecological Modelling*, 124(2–3), 99–119. [https://doi.org/10.1016/S0304-3800\(99\)00156-8](https://doi.org/10.1016/S0304-3800(99)00156-8)
- Cheng, S. J., Bohrer, G., Steiner, A. L., Hollinger, D. Y., Suyker, A., Phillips, R. P., & Nadelhoffer, K. J. (2015). Variations in the influence of diffuse light on gross primary productivity in temperate ecosystems. *Agricultural and Forest Meteorology*, 201, 98–110. <https://doi.org/10.1016/j.agrformet.2014.11.002>
- Cheng, S. J., Steiner, A. L., Hollinger, D. Y., Bohrer, G., & Nadelhoffer, K. J. (2016). Using satellite-derived optical thickness to assess the influence of clouds on terrestrial carbon uptake. *Journal of Geophysical Research: Biogeosciences*, 121, 1747–1761. <https://doi.org/10.1002/2016JG003365>
- Choudhury, B. J. (2000). A sensitivity analysis of the radiation use efficiency for gross photosynthesis and net carbon accumulation by wheat. *Agricultural and Forest Meteorology*, 101(2–3), 217–234. [https://doi.org/10.1016/S0168-1923\(99\)00156-2](https://doi.org/10.1016/S0168-1923(99)00156-2)
- Cirino, G. G., Souza, R. A. F., Adams, D. K., & Artaxo, P. (2014). The effect of atmospheric aerosol particles and clouds on net ecosystem exchange in the Amazon. *Atmospheric Chemistry and Physics*, 14(13), 6523–6543. <https://doi.org/10.5194/acp-14-6523-2014>
- Da Rocha, H. R., Goulden, M. L., Miller, S. D., Menton, M. C., Pinto, L. D. V. O., De Freitas, H. C., & Silva Figueira Am, E. (2004). Seasonality of water and heat fluxes over a tropical forest in eastern Amazonia. *Ecological Applications*, 14(sp4), 22–32. <https://doi.org/10.1890/02-6001>
- Davidson, E. A., De Araujo, A. C., Artaxo, P., Balch, J. K., Brown, I. F., Bustamante, M. M. C., ... Wofsy, S. C. (2012). The Amazon basin in transition. *Nature*, 481(7381), 321–328. <https://doi.org/10.1038/nature10717>
- De Goncalves, L. G., Baker, I., Christoffersen, B., Costa, M., Coupe, N. R., Da Rocha, H., ... Nobre Muza, M. (2010). The Large Scale Biosphere-Atmosphere Experiment in Amazônia, Model Intercomparison Project (LBA-MIP) protocol. Version 4.0.
- De Gonçalves, L. G. G., Borak, J. S., Costa, M. H., Saleska, S. R., Baker, I., Restrepo-Coupe, N., ... Zeng, X. (2013). Overview of the Large-Scale Biosphere-Atmosphere Experiment in Amazonia Data Model Intercomparison project (LBA-DMIP). *Agricultural and Forest Meteorology*, 182–183, 111–127. <https://doi.org/10.1016/j.agrformet.2013.04.030>
- De Pury, D. G. G., & Farquhar, G. D. (1997). Simple scaling of photosynthesis from leaves to canopies without the errors of big-leaf models. *Plant, Cell & Environment*, 20(5), 537–557. <https://doi.org/10.1111/j.1365-3040.1997.00094.x>
- De Weirtd, M., Verbeeck, H., Maignan, F., Peylin, P., Poulter, B., Bonal, D., ... Steppe, K. (2012). Seasonal leaf dynamics for tropical evergreen forests in a process-based global ecosystem model. *Geoscientific Model Development*, 5(5), 1091–1108. <https://doi.org/10.5194/gmd-5-1091-2012>
- Doughty, C. E., Flanner, M. G., & Goulden, M. L. (2010). Effect of smoke on subcanopy shaded light, canopy temperature, and carbon dioxide uptake in an Amazon rainforest. *Global Biogeochemical Cycles*, 24, GB3015. <https://doi.org/10.1029/2009GB003670>
- Doughty, C. E., & Goulden, M. L. (2008). Seasonal patterns of tropical forest leaf area index and CO₂ exchange. *Journal of Geophysical Research*, 113, G00B06. <https://doi.org/10.1029/2007JG000590>
- Falge, E., Baldocchi, D., Tenhunen, J., Aubinet, M., Bakwin, P., Berbigier, P., ... Wofsy, S. (2002). Seasonality of ecosystem respiration and gross primary production as derived from FLUXNET measurements. *Agricultural and Forest Meteorology*, 113, 53–74. [https://doi.org/10.1016/S0168-1923\(02\)00102-8](https://doi.org/10.1016/S0168-1923(02)00102-8)
- Farquhar, G. D., & Roderick, M. L. (2003). Pinatubo, diffuse light, and the carbon cycle. *Science*, 299(5615), 1997–1998. <https://doi.org/10.1126/science.1080681>
- Goulden, M. L., Miller, S. D., Da Rocha, H. R., Menton, M. C., De Freitas, H. C., E Silva Figueira, A. M., & De Sousa, C. A. D. (2004). Diel and seasonal patterns of tropical forest CO₂ exchange. *Ecological Applications*, 14(sp4), 42–54. <https://doi.org/10.1890/02-6008>
- Gu, L. H., Baldocchi, D., Verma, S. B., Black, T. A., Vesala, T., Falge, E. M., & Dowty, P. R. (2002). Advantages of diffuse radiation for terrestrial ecosystem productivity. *Journal of Geophysical Research*, 107(D6), 4050. <https://doi.org/10.1029/2001JD001242>
- Guan, K., Pan, M., Li, H., Wolf, A., Wu, J., Medvigy, D., ... Lyapustin, A. I. (2015). Photosynthetic seasonality of global tropical forests constrained by hydroclimate. *Nature Geoscience*, 8, 284–289. <https://doi.org/10.1038/ngeo2382>
- Guan, K., Wolf, A., Medvigy, D., Caylor, K. K., Pan, M., & Wood, E. F. (2013). Seasonal coupling of canopy structure and function in African tropical forests and its environmental controls. *Ecosphere*, 4(3), art35–art21. <https://doi.org/10.1890/es12-00232.1>
- He, M., Ju, W., Zhou, Y., Chen, J., He, H., Wang, S., ... Zhao, F. (2013). Development of a two-leaf light use efficiency model for improving the calculation of terrestrial gross primary productivity. *Agricultural and Forest Meteorology*, 173, 28–39. <https://doi.org/10.1016/j.agrformet.2013.01.003>
- Houghton, R. A., Lawrence, K. T., Hackler, J. L., & Brown, S. (2001). The spatial distribution of forest biomass in the Brazilian Amazon: A comparison of estimates. *Global Change Biology*, 7(7), 731–746. <https://doi.org/10.1111/j.1365-2486.2001.00426.x>
- Huete, A. R., Didan, K., Shimabukuro, Y. E., Ratana, P., Saleska, S. R., Hutyrá, L. R., ... Myneni, R. (2006). Amazon rainforests green-up with sunlight in dry season. *Geophysical Research Letters*, 33, L06405. <https://doi.org/10.1029/2005GL025583>
- Hutyrá, L. R., Munger, J. W., Saleska, S. R., Gottlieb, E., Daube, B. C., Dunn al, ... Wofsy, S. C. (2007). Seasonal controls on the exchange of carbon and water in an Amazonian rain forest. *Journal of Geophysical Research*, 112, L06405. <https://doi.org/10.1029/2006JG000365>
- Kanniah, K. D., Beringer, J., & Hutley, L. (2013). Exploring the link between clouds, radiation, and canopy productivity of tropical savannas. *Agricultural and Forest Meteorology*, 182–183, 304–313. <https://doi.org/10.1016/j.agrformet.2013.06.010>
- Kim, Y., Knox, R. G., Longo, M., Medvigy, D., Hutyrá, L. R., Pyle, E. H., ... Moorcroft, P. R. (2012). Seasonal carbon dynamics and water fluxes in an Amazon rainforest. *Global Change Biology*, 18, 1322–1334. <https://doi.org/10.1111/j.1365-2486.2011.02629.x>
- Knohl, A., & Baldocchi, D. D. (2008). Effects of diffuse radiation on canopy gas exchange processes in a forest ecosystem. *Journal of Geophysical Research*, 113, G02023. <https://doi.org/10.1029/2007JG000663>
- Kruijt, B., Elbers, J. A., Von Randow, C., Araújo, A. C., Oliveira, P. J., Culf, A., ... Moors, E. J. (2004). The robustness of eddy correlation fluxes for Amazon rain forest conditions. *Ecological Applications*, 14(sp4), 101–113. <https://doi.org/10.1890/02-6004>
- Leuning, R., Zhang, Y. Q., Rajaud, A., Cleugh, H., & Tu, K. (2008). A simple surface conductance model to estimate regional evaporation using MODIS leaf area index and the Penman-Monteith equation. *Water Resources Research*, 44, W10419. <https://doi.org/10.1029/2007WR006562>
- Li, T., Heuvelink, E., Dueck, T. A., Janse, J., Gort, G., & Marcelis, L. F. M. (2014). Enhancement of crop photosynthesis by diffuse light: Quantifying the contributing factors. *Annals of Botany*, 114(1), 145–156. <https://doi.org/10.1093/aob/mcu071>

- Mercado, L. M., Bellouin, N., Sitch, S., Boucher, O., Huntingford, C., Wild, M., & Cox, P. M. (2009). Impact of changes in diffuse radiation on the global land carbon sink. *Nature*, *458*(7241), 1014–1017. <https://doi.org/10.1038/nature07949>
- Monteith, J. L. (1972). Solar radiation and productivity in tropical ecosystems. *Journal of Applied Ecology*, *9*(3), 747–766. <https://doi.org/10.2307/2401901>
- Morton, D. C., Nagol, J., Carabajal, C. C., Rosette, J., Palace, M., Cook, B. D., ... North, P. R. J. (2014). Amazon forests maintain consistent canopy structure and greenness during the dry season. *Nature*, *506*, 221–224. <https://doi.org/10.1038/nature13006>
- Morton, D. C., Rubio, J., Cook, B. D., Gastellu-Etchegorry, J. P., Longo, M., Choi, H., ... Keller, M. (2016). Amazon forest structure generates diurnal and seasonal variability in light utilization. *Biogeosciences*, *13*, 2195–2206. <https://doi.org/10.5194/bg-13-2195-2016>
- Myneni, R. B., Hoffman, S., Knyazikhin, Y., Privette, J. L., Glassy, J., Tian, Y., ... Running, S. W. (2002). Global products of vegetation leaf area and fraction absorbed PAR from year one of MODIS data. *Remote Sensing of Environment*, *83*, 214–231. [https://doi.org/10.1016/S0034-4257\(02\)00074-3](https://doi.org/10.1016/S0034-4257(02)00074-3)
- Nemani, R. R., Keeling, C. D., Hashimoto, H., Jolly, W. M., Piper, S. C., Tucker, C. J., ... Running, S. W. (2003). Climate-driven increases in global terrestrial net primary production from 1982 to 1999. *Science*, *300*, 1560–1563.
- Norman, J. M. (1982). Simulation of microclimates. In I. J. Thomason & J. L. Hatfield (Eds.), *Biometeorology in Integrated Pest Management* (pp. 65–99). New York: Academic Press. <https://doi.org/10.1016/B978-0-12-332850-2.50009-8>
- Priestley, C. H., & Taylor, R. J. (1972). Assessment of surface heat-flux and evaporation using large-scale parameters. *Monthly Weather Review*, *100*(2), 81–92. [https://doi.org/10.1175/1520-0493\(1972\)100%3C0081:OTAOSH%3E2.3.CO;2](https://doi.org/10.1175/1520-0493(1972)100%3C0081:OTAOSH%3E2.3.CO;2)
- Raich, J. W., Rastetter, E. B., Melillo, J. M., Kicklighter, D. W., Steudler, P. A., Peterson, B. J., ... Vorosmarty, C. J. (1991). Potential net primary productivity in south-America—Application of a global model. *Ecological Applications*, *1*(4), 399–429. <https://doi.org/10.2307/1941899>
- Rap, A., Spracklen, D. V., Mercado, L., Reddington, C. L., Haywood, J. M., Ellis, R. J., ... Butt, N. (2015). Fires increase Amazon forest productivity through increases in diffuse radiation. *Geophysical Research Letters*, *42*, 4654–4662. <https://doi.org/10.1002/2015GL063719>
- Restrepo-Coupe, N., Da Rocha, H. R., Hutya, L. R., da Araujo, A. C., Borma, L. S., Christoffersen, B., ... Saleska, S. R. (2013). What drives the seasonality of photosynthesis across the Amazon basin? A cross-site analysis of eddy flux tower measurements from the Brasil flux network. *Agricultural and Forest Meteorology*, *182–183*, 128–144. <https://doi.org/10.1016/j.agrformet.2013.04.031>
- Restrepo-Coupe, N., Levine, N. M., Christoffersen, B. O., Albert, L. P., Wu, J., Costa, M. H., ... Saleska, S. R. (2017). Do dynamic global vegetation models capture the seasonality of carbon fluxes in the Amazon basin? A data-model intercomparison. *Global Change Biology*, *23*(1), 191–208. <https://doi.org/10.1111/gcb.13442>
- Roderick, M. L., Farquhar, G. D., Berry, S. L., & Noble, I. R. (2001). On the direct effect of clouds and atmospheric particles on the productivity and structure of vegetation. *Oecologia*, *129*(1), 21–30. <https://doi.org/10.1007/s004420100760>
- Saleska, S. R., Miller, S. D., Matross, D. M., Goulden, M. L., Wofsy, S. C., da Rocha, H. R., ... Silva, H. (2003). Carbon in Amazon forests: Unexpected seasonal fluxes and disturbance-induced losses. *Science*, *302*, 1554. <https://doi.org/10.1126/science.1091165>
- Saxton, K. E., Rawls, W. J., Romberger, J. S., & Papendick, R. I. (1986). Estimating generalized soil-water characteristics from texture. *Soil Science Society of America Journal*, *50*(4), 1031–1036. <https://doi.org/10.2136/sssaj1986.03615995005000040039x>
- Sellers, P. J., Berry, J. A., Collatz, G. J., Field, C. B., & Hall, F. G. (1992). Canopy reflectance, photosynthesis, and transpiration. III. A reanalysis using improved leaf models and a new canopy integration scheme. *Remote Sensing of Environment*, *42*(3), 187–216. [https://doi.org/10.1016/0034-4257\(92\)90102-P](https://doi.org/10.1016/0034-4257(92)90102-P)
- Von Randow, C., Manzi, O. A., Kruijt, B., Oliveira, A., Zanchi, F. B., Silva, R. L., ... Elbers, J. A. (2004). Comparative measurements and seasonal variations in energy and carbon exchange over forest and pasture in south west Amazonia. *Theoretical and Applied Climatology*, *78*(1–3), 5–26. <https://doi.org/10.1007/s00704-004-0041-z>
- Wild, M. (2012). Enlightening global dimming and brightening. *Bulletin of the American Meteorological Society*, *93*(1), 27–37. <https://doi.org/10.1175/bams-d-11-00074.1>
- Williams, I. N., Riley, W. J., Kueppers, L. M., Biraud, S. C., & Torn, M. S. (2016). Separating the effects of phenology and diffuse radiation on gross primary productivity in winter wheat. *Journal of Geophysical Research: Biogeosciences*, *121*, 1903–1915. <https://doi.org/10.1002/2015JG003317>
- Wu, J., Albert, L. P., Lopes, A. P., Restrepo-Coupe, N., Hayek, M., Wiedemann, K. T., ... Saleska, S. R. (2016). Leaf development and demography explain photosynthetic seasonality in Amazon evergreen forests. *Science*, *351*, 972. <https://doi.org/10.1126/science.aad5068>
- Wu, J., Guan, K., Hayek, M., Restrepo-Coupe, N., Wiedemann, K. T., Xu, X., ... Saleska, S. R. (2016). Partitioning controls on Amazon forest photosynthesis between environmental and biotic factors at hourly to interannual timescales. *Global Change Biology*, *23*(3), 1240–1257. <https://doi.org/10.1111/gcb.13509>
- Yan, H., Wang, S. Q., Billesbach, D., Oechel, W., Bohrer, G., Meyers, T., ... Shugart, H. H. (2015). Improved global simulations of gross primary product based on a new definition of water stress factor and a separate treatment of C3 and C4 plants. *Ecological Modelling*, *297*, 42–59. <https://doi.org/10.1016/j.ecolmodel.2014.11.002>
- Yan, H., Wang, S. Q., Billesbach, D., Oechel, W., Zhang, J. H., Meyers, T., ... Scott, R. (2012). Global estimation of evapotranspiration using a leaf area index-based surface energy and water balance model. *Remote Sensing of Environment*, *124*, 581–595. <https://doi.org/10.1016/j.rse.2012.06.004>
- Yan, H., Wang, S.-Q., Lu, H.-Q., Yu, Q., Zhu, Z. C., Myneni, R. B., ... Shugart, H. H. (2014). Development of a remotely sensing seasonal vegetation-based Palmer Drought Severity Index and its application of global drought monitoring over 1982–2011. *Journal of Geophysical Research: Atmospheres*, *119*, 9419–9440. <https://doi.org/10.1002/2014JD021673>
- Yan, H., Yu, Q., Zhu, Z.-C., Myneni, R. B., Yan, H.-M., Wang, S.-Q., & Shugart, H. H. (2013). Diagnostic analysis of interannual variation of global land evapotranspiration over 1982–2011: Assessing the impact of ENSO. *Journal of Geophysical Research: Atmospheres*, *118*, 8969–8983. <https://doi.org/10.1002/jgrd.50693>
- Yang, W., Shabanov, N. V., Huang, D., Wang, W., Dickinson, R. E., Nemani, R. R., ... Myneni, R. B. (2006). Analysis of leaf area index products from combination of MODIS Terra and Aqua data. *Remote Sensing of Environment*, *104*, 297–312. <https://doi.org/10.1016/j.rse.2006.04.016>
- Zhou, Y., Wu, X., Ju, W., Chen, J. M., Wang, S., Wang, H., ... Varlagin, A. (2016). Global parameterization and validation of a two-leaf light use efficiency model for predicting gross primary production across FLUXNET sites. *Journal of Geophysical Research: Biogeosciences*, *121*, 1045–1072. <https://doi.org/10.1002/2014JG002876>